

The role of a layer in deep neural networks: a Gaussian Process perspective

Oded Ben-David¹ and Zohar Ringel¹

¹*Racah Institute of Physics, The Hebrew University of Jerusalem.*

A fundamental question in deep learning concerns the role played by individual layers in a deep neural network (DNN) and the transferable properties of the data representations which they learn. To the extent that layers have clear roles one should be able to optimize them separately using layer-wise loss functions. Such loss functions would describe what is the set of good data representations at each depth of the network and provide a target for layer-wise greedy optimization (LEGO). Here we introduce the Deep Gaussian Layer-wise loss functions (DGLs) which, we believe, are the first supervised layer-wise loss functions which are both explicit and competitive in terms of accuracy. The DGLs have a solid theoretical foundation, they become exact for wide DNNs, and we find that they can monitor standard end-to-end training. Being highly structured and symmetric, the DGLs provide a promising analytic route to understanding the internal representations generated by DNNs.

I. INTRODUCTION

Several pleasant features underlay the success of deep learning: The scarcity of bad minima encountered in their optimization¹, their ability to generalize well despite being heavily over-parametrized^{2,3} and expressive⁴, and their ability to generate internal representations which generalize across different domains and tasks^{5,6}. Our current understanding of these features is however largely empirical. Thus the important task of designing more robust DNNs which train faster and allow for transfer of knowledge across domains (transfer learning), involves various ad-hoc choices, trial-and-error, and hard to teach craftsmanship.

While training and generalization can be analyzed in the limit of wide networks^{7,8}, the issue of internal representations and transfer learning is inherently depth related. The practical setup of transfer learning^{5,6} (and some semi-supervised learning schemes⁹) typically involves training a DNN on task A with large amounts data (say image classification) cutting and freezing several of the lowest layers of that DNN, adding a smaller DNN on top the these frozen layers, and training it for task B (say localization of objects in images) with a smaller dataset. The fact that transfer learning often works quite well implies that, to some degree, layers in a DNN learn data representations which are "useful", or aid in solving the task, even without very specific knowledge on the particular weights of subsequent layers.

A way of formalizing usefulness of internal representations is to consider layer-wise greedy optimization. Indeed, if weights-specific knowledge of subsequent layers is unimportant, it should be possible to train each layer of the DNN individually. Such optimization should use, at most, knowledge about the architecture of subsequent layers and the task at hand. Thus a set of layer-wise loss functions should exist which depend, at most, on the architecture and the task. Such loss functions would quantify what is the set of useful representations each layer should aim for, thereby quantifying the role of a layer in a DNN. Furthermore, such loss functions would

in principal allow one to determine whether a layer can be successfully transferred by measuring how well these useful representations agree between different architectures and tasks. The ability to draw analytic insights from such layer-wise loss functions depends heavily on how explicit they are. While many ideas for such layer loss functions have been proposed, to the best of our knowledge, the ones which are explicit do not yield state-of-the-art performance and the ones which yield state-of-the-art performance are not explicit (see review below).

How to obtain such explicit loss functions? Here we turn to a recent work analyzing very wide networks¹⁰. This work capitalizes on the fact that in the infinite width limit fully connected DNNs, when marginalized over their internal parameters, behave as Gaussian Processes (GPs). This GP is fully characterized by the covariance-function (K_{xx}) which measures how two different inputs (x, x) correlate at the output of the DNN, when marginalized over the weights' distribution. As Bayesian Inference can be carried exactly on GPs¹¹, one has an analytic handle on Bayesian Inference in wide DNNs. Notably one may worry that infinitely wide DNNs with an infinite number of parameters will be of little use due to over-fitting, however that is not the case in practice. In fact various works show that the wider the network, the better it seems to generalize^{2,3}. Interestingly there is also evidence that GP predictions remain a good approximation even for networks of depth 10000¹² at initialization. Here we seek to leverage this GP viewpoint for constructing layer-wise loss functions.

Our contributions: 1. We derive and test a novel set of explicit supervised layer-wise loss functions, Deep Gaussian Layer-wise losses (DGLs), for fully connected DNNs. The DGLs lead to state-of-the-art performance on MNIST and CIFAR10 when used in LEGO and can also be used to monitor standard end-to-end optimization. The DGLs are architecture dependent but only through a few effective parameters. 2. We analyze in depth the DGL of a pre-classifier layer and use this analysis to shed light on issues with the Information Bottleneck (IB) approach to DNNs. 3. We show that K_{xx} of finite width DNNs agree with those of very wide network

quite well and suggest a fitting ansatz which makes this agreement even tighter. 4. We provide strong evidence that the GP approach to DNNs is an excellent approximation for the behavior of DNNs with widths as small as 20 neurons.

Related work: The idea of analyzing DNNs layer by layer has a long history. Several early successes of deep networks were obtained using LEGO strategies. In particular good generative models of hand-written digits¹³ and phonetics classifiers¹⁴ were trained using an unsupervised (i.e. label unaware) LEGO strategy which for the latter work was supplemented by stochastic gradient descent (SGD) fine-tuning. Following some attempts to perform supervised LEGO¹⁵, the common practice became to use LEGO as a pre-training initialization protocol¹⁶. As simpler initialization protocols came alone¹⁷ SGD on the entire network (end-to-end) became the common practice. More recent works include several implicit loss function based on IB all having in common that an auxiliary DNN has to be trained in order to evaluate the loss as well as . More analytic approaches include a unsupervised LEGO training^{18,19} algorithm followed by a classifier for datasets resembling Gaussian mixtures, a biologically inspired unsupervised algorithm, and target methods where layers are trained to fit to specific targets chosen by a backwards pass on the network²⁰.

II. GAUSSIAN PROCESSES AND FINITE-WIDTH DNNs

Here we briefly survey relevant results on GPs¹¹ and their covariance functions. Gaussian Processes are a generalization of multi-variable Gaussian distributions to a distribution of functions ($z(x)$)¹¹. Being Gaussian they are completely defined by the first and second moments. The first is typically taken to be zero and second is known as the covariance function ($K_{xx'} = E[z(x)z(x')]$, where E denote expectation under the GP distribution). In addition GPs allow for exact Bayesian Inference. An important conceptual step here is to view the function $z(x)$ as an (infinite-dimensional/non-parametric) representation of the model-parameters.

The equivalence between GPs and very wide DNNs stems from the fact that in the infinite width (channel) limit, fully-connected (convolutional) DNNs with uncorrelated prior on the weights ($P(W)$) are equivalent to GPs^{21,22}. Here $z(x)$ becomes the DNN's output and x denotes the input to the DNN. Alternatively stated, the probability distribution on the space of functions generated by a DNN with random weights, is a Gaussian one. Consequently exact Bayesian Inference on such DNNs is possible^{10,21} and explicitly given by

$$K_{xx'} = \int dW P(W) z(x) z(x') \quad (1)$$

$$l_* = \sum_{nm} K(x_*, x_n) [K(D) + \epsilon^2 I]_{nm}^{-1} l_m$$

where x_* is a new datapoint, l_* is the target vector typically chosen as a one-hot encoding of the categorical label, l_m are the training targets, x_n are the training data-points, $[K(D)]_{nm} = K_{x_n, x_m}$ is the covariance-matrix (the covariance-function projected on the training dataset (D)), ϵ^2 is a regulator corresponding to a noisy measurement of $z(x)$, and I is the identity matrix. Notably while not written explicitly, $z(x)$ is W dependent. Some intuition for this formula can be gained by verifying that $x_* = x_q$ yields $l_* = l_q$.

Implicit in the above matrix-inversion is the full Bayesian integration ($\int dW$) over all DNNs weights, weighted by their likelihood given the dataset ($P(W|D)$). Gaussian Processes in which the covariance-function is derived as above from infinite width DNNs are called NNGPs¹⁰.

Several works have noted quantitative and qualitative similarities between end-to-end SGD training and Bayesian Inference^{10,23–26}. In particular for the CIFAR-10 and MNIST datasets, Bayesian predictions and SGD predictions were shown to be in tight agreement¹⁰. Thus we shall assume that NNGP performance is a monotonic function of the average SGD performance for wide DNNs.

Turning away from the infinite width limit, a finite width DNN cannot be viewed as a GP, at least not strictly. However one may still attempt to approximate it using a GP in what can be thought of as a mean-field/Gaussian approximation. The covariance-function of this GP-approximation is $K_{xx'}$, as defined above. If non-Gaussian corrections are small, the performance of Bayesian inference using the GP-approximation would be a monotonic function of SGD performance. We shall assume from now on that $\text{NNGP} \approx \text{SGD}$ with \approx interpreted as a monotonic relation between performances. This assumption would be supported below by our numerical results.

Still an important problem remains which is how to calculate this GP-approximation. Indeed the space of all possible covariance-functions ($K_{xx'}$) for a high dimensional x is huge thus requiring large amounts of data for a proper fit. Here we make the simplifying assumption, inspired by recent results¹², that the approximating GPs have the functional form of the infinite width NNGP with renormalized prior parameters. Conveniently NNGP covariance-functions can be written using an explicit formula which involves the non-linearity of the network, the prior on the weights and biases ($\sigma_W^{2(l)}, \sigma_b^{2(l)}$) at all layers ($l \in \{0, L-1\}$, where L is the DNN depth). Focusing on the case of the commonly used ReLU activations, the resulting approximate covariance-function of a depth L network at infinite width ($K_{xx'}^{(L)}$) is given by the following

recursive relation²¹

$$K_{xx'}^{(l)} = \sigma_b^{2(l)} + \frac{\sigma_w^{2(l)}}{2\pi} \sqrt{K_{xx}^{(l-1)} K_{x'x'}^{(l-1)}} \times \left(\sin(\Theta_{xx'}^{(l-1)}) + [\pi - \cos(\Theta_{xx'}^{(l-1)})] \Theta_{xx'}^{(l-1)} \right) \quad (2)$$

$$\Theta_{xx'}^{(l)} = \arccos \left(\frac{K_{xx'}^{(l)}}{\sqrt{K_{xx}^{(l)} K_{x'x'}^{(l)}}} \right)$$

where $K_{xx'}^{(0)} = \sigma_b^{2(0)} + \sigma_w^{2(0)} x \cdot x'$. As shown in Fig. (1) $K_{xx'}^{(L)}$ where $\sigma_w^{2(l)}, \sigma_b^{2(l)}$ are taken from their microscopic values (MF) or from a fit (FIT), agrees well with the empirical (sampled) covariance-function. We note by passing that similar explicit formula exist also for error-function activations.

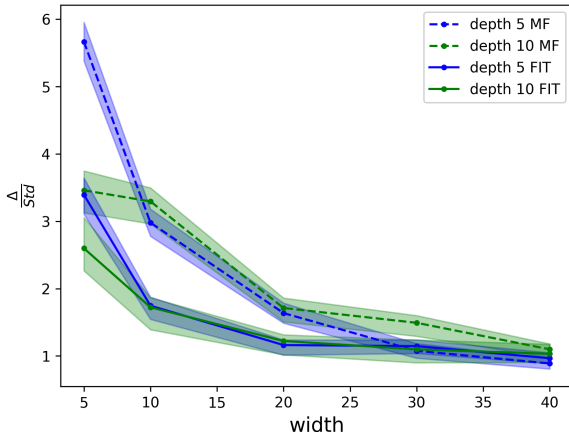


FIG. 1: Accuracy of the mean-field theory (MF) and the mean-field theory with a renormalized prior (FIT) measured in terms of the difference between the sampled covariance function (based on 10000 random weights) and predicted covariance-function divided by sampling noise. The shaded regions are 1std error bars.

III. DERIVING THE DEEP GAUSSIAN LAYER-WISE LOSS FUNCTIONS

To derive the DGL functions let us start with a LEGO strategy which should be optimal in terms of performance yet highly non-explicit (See Fig.2): We begin from the input layer and consider it as our current trainee layer (L_{w^0}). For every set of its parameters (w^0) we perform standard end-to-end training of the entire network between the trainee layer and the classifier (the top-network) with w^0 kept frozen. Next we repeat this training infinitely many times and treat the average performance ($Per(w^0)$) as a loss function for the trainee layer. Then we optimize the parameters such that $w_{opt}^0 = \text{argmin} Per(w^0)$. Subsequently we act on the dataset using $L_{w_{opt}^0}$ to obtain the representation of the dataset in activation space (h_n^0). We then repeat the

process for the $l = 1$ layer with h_n^0 as inputs. This process continues until $l = L - 1$. The last classifier layer is then trained using MSE Loss.

Provided that freezing the parameters of the trainee-layer does not induce optimization issues in the top-network SGD, the above procedure would yield the same performance as average end-to-end SGD. Such optimization issues in the top-network, more well known as co-adaptation issues⁵, arise from tight coupling between top-network and trainee layer weights. They imply that the trainee layer representation learned by standard end-to-end training, is highly correlated with the top-network and thus inadequate for transfer learning⁵.

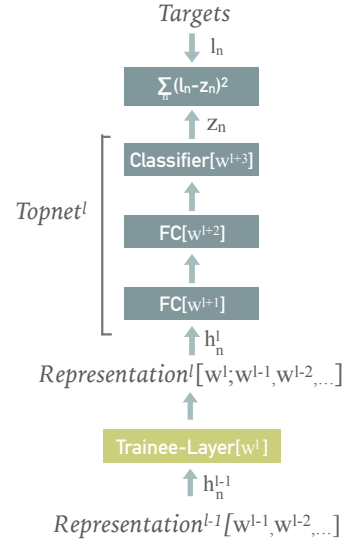


FIG. 2: Layer-wise greedy optimization (LEGO). The l 'th trainee layer, with weights w^l , acts on the $l-1$ representation of the dataset (the output of all previously trained layers). It outputs the l 'th representation which is w^l -dependent. In LEGO we seek to optimize w^l such that this l 'th representation is well classified by the l 'th top-network consisting of all subsequent layers on top of the trainee one. Our strategy is to evaluate this performance by using Bayesian Inference on a Gaussian Process which approximates the function space spanned by the top-network.

Co-adaptation is considered adversarial to learning also outside the scope of LEGO and transfer learning. Indeed the success of dropout regularization is partially associated with its ability to mitigate co-adaptation²⁷. Additionally, co-adaptation being a local minima issue, is more likely to occur away from the over-parametrized regime where modern practical interest lies. We thus make a second assumption which is that co-adaptation effects are small. Note that if co-adaptation is unavoidable one may still group the co-adapting layers into a block of layers and treat this block as an effective layer in the algorithm discussed below.

Assuming no co-adaptation as well as NNGP \approx SGD we shall now derive the DGL functions by approximating $Per[w^l]$ using NNGP Bayesian prediction. To this end let

us either consider a regression problem with data-point (h_n^l) and targets (l_n) or rephrase a classification problem as a regression problem by taking l_n to be a one-hot encoding of the categorical labels. For concreteness we focus on the bottom/input layer (see Fig. 2) which acts on the x_n and maps each to its value in the activation space of the input layer (h_n^0). Consider training the top-network on the dataset represented by (h_n^0, l_n). Taking the GP approximation we consider Eq. (1) with x replaced by h and $K_{xx'}$ replaced by $K_{hh'}$ (the covariance-function of the top-network). The resulting equation now describes how an unseen activation h_* would be classified (l_*) by a trained top-network. To make this into a loss function for the training dataset, rather than for an unseen point, we adopt a leave-one-out cross-validation strategy: We iterate over all data-points, take each one out in turn, treat it as an unseen point, and measure how well we predict its label using the mean Bayesian NNGP prediction.

Assuming K_{nm} has no kernel, taking $\epsilon \rightarrow 0$, and performing some straightforward algebra (see App. I.) the MSE loss of the leave-one-out predictions can be expressed using the inverse of $[K(D)]_{nm}$ over the training dataset ($B_{nm} = [K]_{nm}^{-1}$)

$$L_{DGL} = - \sum_{n,m,q} (l_m \cdot l_n) S_{nm} \quad (3)$$

$$S_{nm} = - \sum_q \frac{B_{nq} B_{qm}}{B_{qq}^2}$$

A few technical comments are in order. The DGL is a function of the trainee layer's parameters via $h_n^l(w^0)$ which enter K_{nm} whose inverse is B_{nm} . Apart from the need to determine the top-networks effective parameters ($\sigma_w^{2(l)}$) numerically or through meta-optimization, the DGL is an explicit function of all the points in the dataset. For the case of ReLU networks without biases, it can be seen from Eq. 2 that all of $\sigma_w^{2(l)}$ collapse into one scale parameter. Lastly we stress that this loss gives a score to a full dataset rather than to points in the dataset.

We turn to discuss the structure and symmetries of L_{DGL} . As L_{DGL} depends on h_n^l only through B_{qp} which in turn depends only on $K(h_q^l, h_p^l)$, it inherits all the symmetries of the latter. For fully connected top-networks it is thus invariant under any orthogonal transformation ($O(d^l)$, where d^l is the dimension of the vector (h_n^l) of the l 'th layer-representation (h_n^l). An additional structure is that L_{DGL} depends on the targets only through the dot-product of the targets which, for the one-hot encoded case, means it is zero unless the labels are equal. The B_{pq} -dependent central piece (S_{nm}) is "unsupervised" or unaware of the labels. It is a negative definite matrix ensuring that the optimal DGL is zero as one expects from a proxy to the MSE loss. One can think of S_{nm} as a measure of sample-similarity-bias of the DNN (more specifically the top-network): when S_{nm} is small (large) for two data-points the networks tends to associate different (similar) targets to them in any classification task.

Crucially S_{nm} is not a simple pairwise dependence on h_n^l, h_m^l , but rather depends on the entire dataset through the covariance-matrix inversion. The DGL function can thus be interpreted as the sample similarity (in the context of the dataset) weighted by the fixed-target similarity.

IV. THE CASE OF A DEPTH ONE NETWORK

It is illustrative to demonstrate our approach on a case where the inversion of the covariance-matrix can be carried out explicitly. To this end we consider a DNN consisting of a fully-connected or convolutional bottom/input layer (L_{w^0}) with weights w^0 and any type of activation. This layer outputs a d dimensional activation vector (h) which is fed into a linear layer with two outputs $\vec{z} = z_1(x), z_2(x)$. We consider a binary regression task with two targets $\vec{z} = \{(1, 0), (0, 1)\}$ which can also be thought of as a binary classification task.

Notably in this shallow scenario many of the assumptions we made in deriving the DGL functions are exact. A linear layer of any width, when marginalized over its weights, is a Gaussian Process whose covariance-function is that of the infinite-width limit. Moreover the loss landscape of an MSE-classifier is convex and therefore co-adaptation effects are absent.

To express the DGL function for this input layer ($L_{DGL@Linear}$), our first task is to find the covariance-function of the top-network namely, the linear layer. Assuming a Gaussian prior of variance σ_w^2 on each of the linear layer's matrix weights and zero bias it is easy to show (App. II.) that

$$K_{hh'} = \sigma_w^2 h \cdot h' \quad (4)$$

$$K_{nm} = \sigma_w^2 H H^T$$

where H is an N by d matrix given by $[H]_{ni} = [h_n^0]_i$.

To facilitate the analysis we next make the assumption that the number of data-points (N) is much larger than the number of labels and also take a vanishing regulator ($\epsilon \rightarrow 0$). As a result we find that the covariance-matrix has a kernel whose dimension is at least $N - d \gg d$. To leading order in d/N one finds that $K^{-1} = (\sigma_w^2 \epsilon)^{-1} P_K$, where P_K is the projector onto the kernel of K_{nm} . This projector is given by (see App. 3)

$$P_K = (I - H \Sigma^{-1} H^T) \quad (5)$$

$$\Sigma = H^T H$$

Indeed one can easily verify that $P_K^2 = P_K$ and that $P_K H H^T = H H^T P_K = 0$ as required. Plugging these results into Eq. 3 one finds that to leading order in N/d

$$L_{DGL@Linear} = \sum_n |l_n|^2 - \sum_{nm} (l_n \cdot l_m) [H \Sigma^{-1} H^T]_{nm} \quad (6)$$

The above equation tell us how to train a layer whose output (H) gets fed into a linear classifier. Let us first discuss its symmetry properties. The first term in this equation is constant under the optimization of w^0 hence we may discard it. The second term is invariant under any rotation (O) of the dataset in activation space ($H \rightarrow HA$). Indeed such transformations can be carried by the classifier itself and hence such changes to the dataset should not affect the performance of the classifier. A bit unexpected is that $L_{DGL@Linear}$ is also invariant under the bigger group of invertible linear transformation ($GL(d)$). While a generic classifier can indeed undo any linear transformation, the prior we put on its weights limits the extent to which it can undo a transformation with vanishing eigenvalues. This enhanced symmetry is a result of taking the $\epsilon \rightarrow 0$ limit, which allows the Gaussian Process to distinguish vanishingly small difference in $z(x_n)$. In practice finite ϵ is often needed for numerical stability and this breaks the $GL(d)$ symmetry down to an $O(d)$ symmetry.

Next we discuss how $L_{DGL@Linear}$ sees the geometry of the dataset. Notably Σ is the covariance matrix of the dataset in activation space. Since it is positive definite we can write $\Sigma = \sqrt{\Sigma}\sqrt{\Sigma}$, $\Sigma^{-1} = \sqrt{\Sigma^{-1}}\sqrt{\Sigma^{-1}}$ and therefore $H\Sigma^{-1}H^T = H\sqrt{\Sigma^{-1}}\sqrt{\Sigma^{-1}}H^T$. We then define $\tilde{H} = H\sqrt{\Sigma^{-1}}$ as the normalized dataset. Indeed its covariance matrix ($\tilde{H}^T\tilde{H}$) is the identity. Thus, $L_{DGL@Linear} = const - \sum_{nm} l_n \cdot l_m \tilde{H}_n \tilde{H}_m$. In these coordinates the loss is a simple pairwise interaction between *normalized datapoints* which tends to make points with equal (opposite) labels closer (far-apart). It thus favors a formation of separate droplets in the normalized representation as illustrated in Fig. 3 panel (B).

The fact that it encourages droplets in the normalized representation rather than in the representation itself is very sensible. Indeed the classifier's performance is a measure of the linear separability of the dataset. This means that points with opposite labels should be on opposite sides of a hyper-plane. However no further improvement in train performance is gained by making equal label points closer in Euclidean distance. Hence pairwise interaction (encouraging high dot-product between similar labels) without normalization is unlikely to be faithful measure of linear separability. Once the dataset is normalized this spread over the directions along the hyper-plane is made to be of order one, hence equal label points do look like they bunch together into droplets (See Fig. 3). In fact based on the above symmetry discussion one finds that $L_{DGL@Linear}$ favors any geometry given by any invertible linear transformation acting on a dataset representation consisting of two well separated droplets. This is a sensible measure of linear separability for generic datasets.

V. CONTRAST WITH INFORMATION BOTTLENECK APPROACHES

It is interesting to compare $L_{DGL@Linear}$ with a different loss function drawn from recent works on the information bottleneck (IB)^{28,29}. In those works it was argued that the role of a layer was to compress the layers representation while maintaining the information on the labels. Formally this means minimizing the mutual information quantity

$$L_{IB} = I(h; x) - \beta I(x; l) \quad (7)$$

for large β . A subtle yet important issue here is the fact that for deterministic networks these mutual information quantities are either constant or infinite depending how one views the entropy of a point. To overcome this the original works used binning of some linear dimension ($l_b \ll 1$) in activation space and other works added a Gaussian noise of variance η^2 to h_n^l ³⁰. In case in which three data-points becoming l_b - or $\sqrt{\eta^2}$ -close are rare, both regularization schemes effectively lead to a pairwise interaction between data-points^{31,32} (see also App. 2.). Notably this is almost always the case at high dimension or when the regulator is taken to zero. For the Gaussian regulator the resulting loss is particularly simple and given by (see App. 2.)

$$L_{IB,\beta} = \sum_{nm} [\beta(1 - l_n l_m) - 1] \Delta S_\eta(|h_n - h_m|) \quad (8)$$

where $\Delta S_\eta(l)$ is an Gaussianly decaying interaction on the scale of $\sqrt{\eta^2}$ given explicitly by the difference in entropy between two d -dimensional Gaussian distribution of variance η^2 and a mixture of such Gaussians as distance l .

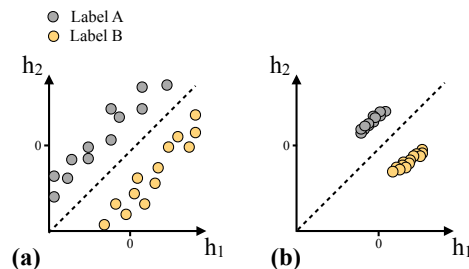


FIG. 3: Two pre-classifier data representations. (a) A typical pre-classifier dataset representation. (b) Droplet formation encouraged by Information Bottleneck loss. The DGL before the classifier seems to capitalize on the fact that both plots are related through normalizing the axis by the co-variance matrix.

At the input of the linear classifier, one can easily see the differences between the layer-representations favored by $L_{IB,\beta}$ and by $L_{DGL@Linear}$ (see Fig. 3). The former, being unaware of the classifier or the architecture, simply encourages the formation of droplets which, as

argued previously, are not a faithful measure of linear separability. To achieve this unnecessary goal it is likely to compromise on the margin. The latter being aware of the classifier, encourages linear separability. We conclude that $L_{IB,\beta}$ is unlikely to be a good layer-wise loss function close to the classifier. This lack of architecture awareness of IB (regulated using binning or Gaussian noise) is generally concerning.

VI. NUMERICAL TESTS

Here we report several numerical experiments aimed at testing whether the DGLs can monitor standard end-to-end optimization and measure the effectiveness of the DGL functions in LEGO. Experiments were conducted on three datasets: MNIST with 10k training samples randomly selected from the full MNIST training set and balanced to have an equal number of samples from each label (MNIST_{10k}), CIFAR10 with 10k training samples similarly selected and balanced in terms of labels (CIFAR10_{10k}). Binary MNIST with only the digits 1 and 7 and 2k training samples (BMNIST_{2k}), similarly selected and balanced in terms of labels. For each dataset, an additional validation set of size equal to the training set, was randomly selected from the full respective training set, excluding the samples selected for the training set. The validation set was balanced in terms of labels. For MNIST_{10k} and CIFAR10_{10k} the reported test set was the respective standard test-set and for BMNIST_{2k} the reported test set was the samples from the standard test-set with labels 1 and 7. The test sets were not balanced in terms of labels.

All experiments were conducted using fully-connected DNNs, with depth L , consisting of L activated layers with fixed width (d) and a linear classifier layer with output dimension given by the number of classes. The targets were zero-mean one-hot encoded in all experiments except for CIFAR10_{10k}, where the labels were one-hot encoded. The loss function for all non-DGL training was MSE loss.

For each dataset we conducted the following procedure: 1. End-to-end SGD training under MSE loss 2. Evaluation of the mean-field covariance function of the end-to-end-trained network 3. DGL-Monitored end-to-end SGD training under MSE loss with the same hyperparameters as in step 1. and with the mean-field covariance function evaluated at step 2. 4. LEGO training of all activated layers under DGL, using the mean-field covariance function evaluated at step 2. The activated layers were optimized sequentially, starting from the inputs layer. Each layer was optimized once, then kept frozen during the optimization of subsequent layers. 5. Training of the linear classifier layer only, under MSE loss, with the activated layers frozen, either at the DGL-optimized weights or at the randomly-initialized values.

End-to-end training was done using either vanilla SGD optimizer (BMNIST_{2k}) or Adam optimizer

TABLE I: Test accuracy of LEGO with DGL compared with other approaches.

Dataset	L/d	End-to-end	DGL	Random
MNIST _{10k}	2/2000	97.71	97.18	94.42
MNIST _{10k}	3/1000	96.59	97.15	92.18
CIFAR10 _{10k}	5/2000	45.40	47.45	34.28
BMNIST _{2k}	2/20	98.52	99.26	87.29
BMNIST _{2k}	3/20	98.61	99.21	93.52

(CIFAR10_{10k}, MNIST_{10k}) with standard internal parameter. All DGL training was done using the Adam optimizer with standard internal parameters. All training was done with fixed learning rates lr and weight decay, wd . lr and wd were manually selected for each step in each dataset. The best hyper parameters for each step were selected for minimal loss on the validation set.

DGL Monitoring. Figure (4) shows DGL monitoring of end-to-end training (step 2.) of a network with $(L, d) = (3, 20)$. Even at this small width, DGL tracks end-to-end training very well. Various finer details are discussed in the caption.

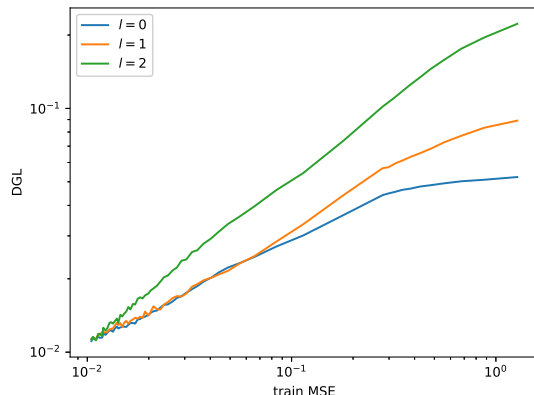


FIG. 4: Monitoring end-to-end SGD training using DGL for BMNIST_{2k} with 3 activated layers of width 20. A monotonic behavior of DGLs versus training MSE loss is apparent. Notably all layers converged to similar DGL values which are close to the training MSE values. In addition the ordering of DGLs for the layers is ascending. Both are expected since DGL predicts the accuracy given that subsequent layers have been trained.

DGL LEGO. Table I shows the test performances of steps 4.& 5., on the three aforementioned datasets for several L and d choices. End-to-end test accuracy is taken from Ref. [10] apart from BMNIST_{2k} where we report the test accuracy obtained at step 1. end-to-end training. The Random column serves as a simple baseline for the effect of depth where we take the randomly initialized network and freeze the weights of all layers apart from the linear classifier.

VII. DISCUSSION

Following recent works on the Information Bottleneck (IB) theory of deep learning^{28,29} there has been a surge of works analyzing the layer representations generated by deep neural networks from both a geometrical and an information theory viewpoint. In this work we argued, both theoretically and numerically, that one can formalize what constitutes a good layer representation explicitly using a set of loss functions—the DGL functions. These loss functions differ from the losses implied by IB in many aspects but mainly, in the fact that they are aware of the architecture of the network. We argued that this is essential, at least close to the classifier.

The DGL functions are well capable of monitoring the optimization of end-to-end training in a layer-wise fashion. Moreover they enable a competitive layer by layer optimization of the network. Although such training is admittedly slower, it has the advantage of generating layer representations with no co-adaptation effects which

are likely to be better for transfer learning⁵.

To the best of our knowledge our LEGO approach outperforms all other explicit LEGO approaches (i.e ones which do not require auxiliary DNNs). Nevertheless our aim here is not to provide a more powerful algorithm for optimization. Rather, we wish to open an analytic window to the incremental role of DNN layers and the representations they learn. Indeed the explicit nature of the DGL functions combined with their high level of structure, symmetry, and empirical accuracy, invites further study regarding the interpretability of layer representations. Understanding these representations would help unravel the inner workings of DNNs and facilitate their use in a more modular fashion across different domains.

Bibliography

- ¹ F. Draxler, K. Veschgini, M. Salmhofer, and F. A. Hamprecht, arXiv e-prints arXiv:1803.00885 (2018), 1803.00885.
- ² B. Neyshabur, Z. Li, S. Bhojanapalli, Y. LeCun, and N. Srebro, arXiv e-prints arXiv:1805.12076 (2018), 1805.12076.
- ³ B. Neyshabur, R. Tomioka, and N. Srebro, arXiv e-prints arXiv:1412.6614 (2014), 1412.6614.
- ⁴ C. Zhang, S. Bengio, M. Hardt, B. Recht, and O. Vinyals, arXiv e-prints arXiv:1611.03530 (2016), 1611.03530.
- ⁵ J. Yosinski, J. Clune, Y. Bengio, and H. Lipson, in *Proceedings of the 27th International Conference on Neural Information Processing Systems - Volume 2* (MIT Press, Cambridge, MA, USA, 2014), NIPS'14, pp. 3320–3328, URL <http://dl.acm.org/citation.cfm?id=2969033.2969197>.
- ⁶ P. Sermanet, D. Eigen, X. Zhang, M. Mathieu, R. Fergus, and Y. LeCun, arXiv e-prints arXiv:1312.6229 (2013), 1312.6229.
- ⁷ S. Mei, A. Montanari, and P.-M. Nguyen, *Proceedings of the National Academy of Sciences* **115**, E7665 (2018), ISSN 0027-8424, <https://www.pnas.org/content/115/33/E7665.full.pdf>, URL <https://www.pnas.org/content/115/33/E7665>.
- ⁸ G. De Palma, B. Toussi Kiani, and S. Lloyd, arXiv e-prints arXiv:1812.10156 (2018), 1812.10156.
- ⁹ D. P. Kingma, S. Mohamed, D. Jimenez Rezende, and M. Welling, in *Advances in Neural Information Processing Systems 27*, edited by Z. Ghahramani, M. Welling, C. Cortes, N. D. Lawrence, and K. Q. Weinberger (Curran Associates, Inc., 2014), pp. 3581–3589, URL <http://papers.nips.cc/paper/5352-semi-supervised-learning-with-deep-generative-models.pdf>.
- ¹⁰ J. Lee, J. Sohl-dickstein, J. Pennington, R. Novak, S. Schoenholz, and Y. Bahri, in *International Conference on Learning Representations* (2018), URL <https://openreview.net/forum?id=B1EA-M-OZ>.
- ¹¹ C. E. Rasmussen and C. K. I. Williams, *Gaussian Processes for Machine Learning (Adaptive Computation and Machine Learning)* (The MIT Press, 2005), ISBN 026218253X.
- ¹² L. Xiao, Y. Bahri, J. Sohl-Dickstein, S. S. Schoenholz, and J. Pennington, arXiv e-prints arXiv:1806.05393 (2018), 1806.05393.
- ¹³ G. E. Hinton, S. Osindero, and Y.-W. Teh, *Neural Computation* **18**, 1527 (2006), pMID: 16764513, <https://doi.org/10.1162/neco.2006.18.7.1527>, URL <https://doi.org/10.1162/neco.2006.18.7.1527>.
- ¹⁴ A. Mohamed, G. E. Dahl, and G. Hinton, *IEEE Transactions on Audio, Speech, and Language Processing* **20**, 14 (2012), ISSN 1558-7916.
- ¹⁵ Y. Bengio, P. Lamblin, D. Popovici, and H. Larochelle, in *Proceedings of the 19th International Conference on Neural Information Processing Systems* (MIT Press, Cambridge, MA, USA, 2006), NIPS'06, pp. 153–160, URL <http://dl.acm.org/citation.cfm?id=2976456.2976476>.
- ¹⁶ Y. LeCun, Y. Bengio, and G. Hinton, *Nature* **521**, 436 EP (2015), URL <http://dx.doi.org/10.1038/nature14539>.
- ¹⁷ X. Glorot and Y. Bengio, in *Proceedings of the thirteenth international conference on artificial intelligence and statistics* (2010), pp. 249–256.
- ¹⁸ J. Kadmon and H. Sompolinsky, in *Advances in Neural Information Processing Systems 29*, edited by D. D. Lee, M. Sugiyama, U. V. Luxburg, I. Guyon, and R. Garnett (Curran Associates, Inc., 2016), pp. 4781–4789.
- ¹⁹ R. Meir and E. Domany, *Phys. Rev. A* **37**, 608 (1988), URL <https://link.aps.org/doi/10.1103/PhysRevA.37.608>.
- ²⁰ D.-H. Lee, S. Zhang, A. Fischer, and Y. Bengio, arXiv e-prints arXiv:1412.7525 (2014), 1412.7525.
- ²¹ Y. Cho and L. K. Saul, in *Proceedings of the 22Nd International Conference on Neural Information Processing Systems* (Curran Associates Inc., USA, 2009), NIPS'09, pp. 342–350, ISBN 978-1-61567-911-9, URL <http://dl.acm.org/citation.cfm?id=2984093.2984132>.

- ²² R. Novak, L. Xiao, J. Lee, Y. Bahri, G. Yang, D. A. Abolafia, J. Pennington, and J. Sohl-Dickstein, arXiv e-prints arXiv:1810.05148 (2018), 1810.05148.
- ²³ M. Welling and Y. W. Teh, in *Proceedings of the 28th International Conference on International Conference on Machine Learning* (Omnipress, USA, 2011), ICML'11, pp. 681–688, ISBN 978-1-4503-0619-5, URL <http://dl.acm.org/citation.cfm?id=3104482.3104568>.
- ²⁴ S. Mandt, M. D. Hoffman, and D. M. Blei, ArXiv e-prints (2017), 1704.04289.
- ²⁵ A. Jacot, F. Gabriel, and C. Hongler, ArXiv e-prints (2018), 1806.07572.
- ²⁶ P. Chaudhari and S. Soatto, in *International Conference on Learning Representations* (2018), URL <https://openreview.net/forum?id=HyWrIgWOW>.
- ²⁷ N. Srivastava, G. Hinton, A. Krizhevsky, I. Sutskever, and R. Salakhutdinov, J. Mach. Learn. Res. **15**, 1929 (2014), ISSN 1532-4435, URL <http://dl.acm.org/citation.cfm?id=2627435.2670313>.
- ²⁸ N. Tishby and N. Zaslavsky, ArXiv e-prints (2015), 1503.02406.
- ²⁹ R. Shwartz-Ziv and N. Tishby, ArXiv e-prints (2017), 1703.00810.
- ³⁰ A. M. Saxe, Y. Bansal, J. Dapello, M. Advani, A. Kolchinsky, B. D. Tracey, and D. D. Cox, in *International Conference on Learning Representations* (2018), URL https://openreview.net/forum?id=ry_WPG-A-.
- ³¹ A. Kolchinsky and B. D. Tracey, Entropy **19** (2017), ISSN 1099-4300, URL <http://www.mdpi.com/1099-4300/19/7/361>.
- ³² Z. Goldfeld, E. van den Berg, K. Greenewald, I. Melnyk, N. Nguyen, B. Kingsbury, and Y. Polyanskiy, arXiv e-prints arXiv:1810.05728 (2018), 1810.05728.
- ³³ R. Rifkin and A. Klautau, J. Mach. Learn. Res. **5**, 101 (2004), ISSN 1532-4435, URL <http://dl.acm.org/citation.cfm?id=1005332.1005336>.
- ³⁴ A. (under double blind review <https://openreview.net/forum?id=r1Nb5i05tX>) (2018), URL <https://openreview.net/forum?id=r1Nb5i05tX>.

Appendix A: Derivation of the DGL functions

Here we consider a multi-label classification dataset (D) consisting of N data points each described by a d dimensional vector x_n and a "one-hot two dimensional label (target) vector ($l = \{(1, 0, \dots), (0, 1, \dots), \dots\}$) for each class. As in^{10,33} we treat classification as a regression task where the network's outputs for a given class are optimized to be close to the one-hot label (MSE loss).

Next we define the n -left-out dataset (D_n) consisting of all points except the point n . Our starting point for defining the DGL is the Bayesian prediction formula for the label vector (l_n^*) of an unseen datapoint (x_n) (unseen with respect to $\{rmD_n\}$)

$$l_n^* = \sum_{qp} [K(D)]_{nq} [\{B(D_n)\}^n]_{qp} l_p \quad (A1)$$

$$[\{A\}^n]_{pq} \equiv \begin{cases} A_{pq} & p \neq n \text{ and } q \neq n, \\ 0 & \text{otherwise.} \end{cases}$$

where $K(D)_{pq} = K(x_p, x_q)$ is the covariance function projected on the dataset D, $B(D_n) = [K(D_n) + \epsilon^2 I_{N-1}]^{-1}$ where $K(D_n)$ is the (n, n) -minor of $K(D)$ or equivalently the covariance-function projected onto D_n , and I_{N-1} is the identity matrix in an $N-1$ dimensional space. Note that we choose indices to remain faithful to data-points, so that the indices of $K(D_n)$ are chosen to be the set $\{1, \dots, n-1, n+1, \dots, N\}$ rather than $\{1..N-1\}$.

It would be convenient both analytically and numerically to relate $B(D_n)$ and $B(D) = [K(D) + \epsilon^2 I_N]^{-1}$. To this end we employ a relation between inverse of a positive definite matrix (Q) and its (n, n) -minor (Q_n)

$$[Q_n^{-1}]_{pq} = [Q^{-1}]_{pq} - \frac{[Q^{-1}]_{pn}[Q^{-1}]_{nq}}{[Q^{-1}]_{nn}} \quad (A2)$$

$$[\{Q_n^{-1}\}^n]_{pq} = [Q^{-1}]_{pq} - \frac{[Q^{-1}]_{pn}[Q^{-1}]_{nq}}{[Q^{-1}]_{nn}}$$

Notably since Q is positive definite and bounded, Q^{-1} is also positive definite and so the above denominator is always nonzero. Note that since $K(D)$ is semi-positive-definite $K(D) + \epsilon^2 I$ is positive-definite. The difference on the r.h.s. of both of the above two equations lays solely in allowed values of p, q ($\{1, \dots, n-1, n+1, \dots, N\}$ for the first Eq. and $\{1, \dots, N\}$ for second).

Following this one can show that

$$K(D_n)B(D_n) = I_{N-1} - \epsilon^2 B(D_n) \quad (A3)$$

$$= \lim_{\epsilon \rightarrow 0} I - P_{Ker[K(D_n)]} = P_{Im[K(D_n)]}$$

$$[K(D)\{B(D_n)\}^n]_{pq} = \delta_{pq} - \epsilon^2 [B(D)]_{pq}$$

$$- \delta_{pn} \frac{[B(D)]_{nq}}{[B(D)]_{nn}} + \epsilon^2 \frac{[B(D)]_{pn}[B(D)]_{nq}}{[B(D)]_{nn}}$$

$$= \lim_{\epsilon \rightarrow 0} \delta_{pq} - \delta_{pn} \frac{[B(D)]_{nq}}{[B(D)]_{nn}}$$

$$- \left(P_{Ker[K(D_n)]} \right)_{pq} - \frac{[P_{Ker[K(D_n)]}]_{pn}[P_{Ker[K(D_n)]}]_{nq}}{[P_{Ker[K(D_n)]}]_{nn}}$$

where P_V is the projector onto the subspace V , $Ker[K(D_n)]$ is the kernel subspace of $K(D_n)$, and $Im[K(D_n)]$ is the image subspace of $K(D_n)$.

Turning to the variance in the predicted target vector (l_n^*) the standard formula gives¹¹

$$K_n^* = [K(D)]_{nn} - \sum_{pq} [K(D)]_{np} [\{B(D_n)\}^n]_{pq} [K(D)]_{qn} \quad (A4)$$

which using the above relations gives

$$K_n^* = \frac{1}{[B(D)]_{nn}} - \epsilon^2 \quad (A5)$$

note that since $B(D)$ is positive definite with maximal eigenvalue of $1/\epsilon^2$ we get that $[B(D)]_{nn} < 1/\epsilon^2$ and therefore the variance is non-negative as required.

We next define the DGL function as the MSE loss of the Bayesian prediction

$$L_{DGL} = \sum_n |l_n^* - l_n|^2 \quad (A6)$$

Notably one can also add the variance ($\sum_n K_{nn}$) to this expression making it a more accurate measure of the expected MSE loss. For simplicity and since we found that it makes little difference in practice we did so in the text. The Github repository we opened has this option available. In the generic case in which the covariance-matrix has no kernel and taking the limit of zero ϵ we obtain

$$L_{DGL} = \sum_n \frac{\sum_{q,p} [B(D)]_{qn} [B(D)]_{np} (l_q \cdot l_p)}{[B(D)]_{nn}^2} \quad (A7)$$

Appendix B: Information Bottleneck from the Pair Distribution Function.

The Information Bottleneck (IB) approach asserts^{28,29} that each layer, having activations T , minimizes the loss function $I(X : T) - \beta I(Y : T)$, where $I(X : T)$ ($I(Y : T)$) is the mutual information between the activations and the input (label) and β is an undetermined layer specific constant which is usually order of a 100²⁹. Notably IB was proposed for deterministic network in which T is a deterministic function of X . As commented in many works^{30,31}, in such settings mutual information quantities are ill defined and require a regulator. The regulator defines how much information is in one data-point and how close two points have to be to collapse into one point. One type of regulator several authors recommend^{30,34}, consists of adding a very small Gaussian random noise ϵ to T and using that perturbed $T + \epsilon$ in the above loss.

For ϵ much smaller than the typical inter-datapoint spacing and at high dimension, one can fairly assume that pairs of data-points coming ϵ close in the space of activations cause the vast majority of information loss whereas triplets of the datapoints coming ϵ close are far more rare. Clearly for low enough ϵ (i.e the deterministic limit) it would always be true unless three points happen to collapse exactly on one another. Taking this as our prescription for determining ϵ , we show below that mutual information becomes a property of the pair-distribution-function (PDF) of the dataset (defined below) and as a result the IB compression can be measured only through knowledge of the pair-wise distances between all points. Such PDFs were analyzed in Ref.³² and indeed compression (following auxiliary noise addition) was linked to reduction of pairwise distance in these PDFs.

We turn to establish the mapping between mutual information with a small ϵ -noise regulator and the pair-distribution function. For brevity we focus only on $I(T + \epsilon : X)$. We make the reasonable assumption that data-points (x_n) have no repetitions and are all equally likely. Using $I(T + \epsilon : X) = H(T + \epsilon) - H(T + \epsilon | X)$ we first

find that the second contribution is just the entropy of ϵ ($H(\epsilon)$). The latter is d -dimensional Gaussian distribution with variance σ_ϵ , which we denote by $H(\epsilon)$. The former is the entropy of $T + \epsilon$. In cases where all data-points in T space ($h_n = T(x_n)$) are much further apart on the scale of σ_ϵ entropy becomes that of choosing a data-point ($\log(N) = H(X)$, where N is the number of datapoints) plus that a single datapoint $H(T + \epsilon) = H(X) + H(\epsilon)$. This implies that $I(T + \epsilon : X) = H(X)$ as expected in this limit. Next consider the case where some points are far apart but some point are bounded to pairs. The entropy is now given by

$$H(T + \epsilon : X) = \log(N) + H(\epsilon) + \frac{2}{N} \sum_p [H(\Delta_p; \sigma_\epsilon) - H(\infty; \sigma_\epsilon)] \quad (B1)$$

where p runs over all pairs, Δ_p is the distance between members of the pair, and $H(\Delta_p; \sigma_\epsilon)$ is the entropy of mixture of two d-dimensional Gaussians with variance σ_ϵ at distance Δ_p . Noting that $[H(\Delta; \sigma_\epsilon) - H(\infty; \sigma_\epsilon)]$ decays as $e^{-\Delta^2/\sigma_\epsilon^2}$ one can just as well extend this sum over pairs to a sum over all points finally arriving at

$$H(T + \epsilon : X) = \log(N) + H(\epsilon) + \frac{1}{N} \sum_{n,m} [H(t_n - t_m; \sigma_\epsilon) - H(\infty; \sigma_\epsilon)] \quad (B2)$$

A summation of two particles/data-points terms as the one above can always be expressed using the pair-distribution-function (PDF) whose standard definition is

$$PDF_{all}(r) = \frac{1}{N(N-1)} \sum_{n \neq m} \delta(|h_n - h_m| - r) \quad (B3)$$

it is then easy to verify that

$$I(T + \epsilon : X) = \log(N) + (N-1) \int dr PDF_{all}(r) [H(r; \sigma_\epsilon) - H(\infty; \sigma_\epsilon)] \quad (B4)$$

Similarly $I(T + \epsilon : Y)$ can be expressed using the opposite-label PDF given by

$$PDF_{+-}(r) = \frac{4}{N^2} \sum_{n,m*} \delta(|h_n - h_{m*}| - r) \quad (B5)$$

$$I(T + \epsilon : Y) = \log(N) + \frac{N}{2} \int dr PDF_{+-}(r) [H(r; \sigma_\epsilon) - H(\infty; \sigma_\epsilon)]$$

where n and m^* scan data-points with opposite labels. We thus conclude that optimization the IB functional following ϵ -noise regularization, either in the limit of $\epsilon \rightarrow 0$ or in the limit where three points reaching a distance of ϵ are rare, is simply a particular type of label dependent pairwise interaction.

Appendix C: DGL for the pre-classifier layer

Here we derive in detail the DGL of pre-classifier layer. The inverse of $K_{nm} + \epsilon^2 \mathbf{I}$. This matrix is defined by

$$B_{nm} = (\sigma_w H H^T + \epsilon^2 \mathbf{I})^{-1} \quad (\text{C1})$$

where we recall that H is an N by d given by $[H]_{ni} = h_i(x_n) = [L_W(x_n)]_i$. Taking the limit of $\epsilon \rightarrow 0$ one immediately has that

$$B_{nm} = \frac{1}{\epsilon^2} P_{\text{Ker}[HH^T]} + O(\epsilon^0) \quad (\text{C2})$$

Without fine tuning $\Sigma = H^T H$ is positive-definite. Notably this statement is equivalent to saying that the $N \times d$ matrix H has d linearly independent columns. Notably when $N \geq d$ having two linearly dependent columns requires fine-tuning of $N - d + 1$ parameters, hence when $N \gg d$ this becomes extremely unlikely under any reasonable ensemble for H .

In this case one can show that $P_{\text{Ker}[HH^T]} = I - H \Sigma^{-1} H^T$. Indeed

$$P_{\text{Ker}[HH^T]}^2 = I - 2H \Sigma^{-1} H^T + H \Sigma^{-1} H^T H \Sigma^{-1} H^T \quad (\text{C3})$$

$$= I - 2H \Sigma^{-1} H^T + H \Sigma^{-1} H^T$$

$$= P_{\text{Ker}[HH^T]}$$

$$H H^T P_{\text{Ker}[HH^T]} = 0 \quad (\text{C4})$$

$$[I - P_{\text{Ker}[HH^T]}] H H^T = H H^T \quad (\text{C5})$$

This equation implies that $P_{\text{Ker}[HH^T]}$ is a projector (in fact an Hermitian projector as is easy to verify). The second that its image is in the kernel of $H H^T$. The third that its kernel is in the image of $H H^T$. All in all it implies that it is a projector whose image coincides with the kernel of $H H^T$ as required.

Next we consider Eqs. (A3). The fact that the kernel is non-trivial adds several complicated terms to our loss. These all term depend on $[P_{\text{Ker}[HH^T]}]_{pq}$ which we next expand as

$$[P_{\text{Ker}[HH^T]}]_{pq} = \delta_{pq} - [P_{\text{Im}[HH^T]}]_{pq} = \delta_{pq} + O(d/N). \quad (\text{C6})$$

we in the right hand side we noted that $\text{Im}[HH^T]$, the image of $H H^T$, is of dimension $d \ll N$, consequently the norm of the operator $[P_{\text{Im}[HH^T]}]_{pq}$ is d , while the norm of the δ_{pq} is N . Notably this statement is only accurate element-wise when we assume that $P_{\text{Im}[HH^T]}$ has no particular relation with the basis on which the matrix is written on. For this not to hold it would require that at least one d -dimensional row of H is orthogonal to all the remaining $N - 1$ rows. This is again exponentially unlikely in the limit of $N \gg d$ under any reasonable ensemble for H .

Accordingly we treat the expansion in the d/N as an expansion in $P_{\text{Im}[HH^T]} = H \Sigma^{-1} H^T$. For instance we can

then expand

$$\begin{aligned} \sum_n \frac{[B(\mathbf{D})]_{pn} [B(\mathbf{D})]_{nq}}{[B(\mathbf{D})]_{nn}^2} &= \sum_n \frac{[B(\mathbf{D})]_{pn} [B(\mathbf{D})]_{nq}}{1 + O(d/N)} \\ &= P_{\text{Ker}[HH^T]} + O((d/N)^2) \end{aligned} \quad (\text{C7})$$

Plugging this into Eq. (A7) we obtain

$$L_{\text{DGL@Linear}} = \sum_n |l_n|^2 - \sum_{nm} [H \Sigma^{-1} H^T]_{nm} (l_n \cdot l_m) \quad (\text{C8})$$

as in the main text.